Macromolecular Research, Vol. 20, No. 12, pp 1300-1306 (2012)
DOI 10.1007/s13233-012-0203-2

www.springer.com/13233
pISSN 1598-5032 eISSN 2092-7673

Compatibility and Physical Properties of Poly(lactic acid)/ Poly(ethylene terephthalate glycol) Blends

Jun Yong Park[1], Sung Yeon Hwang[2], Won Jae Yoon[1], Eui Sang Yoo[3], and Seung Soon Im*[,1]

[1]Department of Organic and Nano Engineering, College of Engineering, Hanyang University, Seoul 133-791, Korea
[2]SKC Advanced Technology R&D Center #911, Gyeonggi 440-301, Korea
[3]KITECH Textile Ecology Laboratory, Gyeonggi 426-170, Korea

Received April 27, 2012; Revised April 30, 2012; Accepted June 1, 2012

Abstract: Blends of poly(lactic acid) (PLA) and poly(ethylene terephthalate glycol) (PETG) of various compositions were prepared by melt compounding and their compatibilities, physical properties, and isothermal crystallization behaviors were investigated. The calculated solubility parameters of PETG are similar to those of PLA. The interaction parameter between PLA and PETG was derived from the Flory-Huggins theory and predicted that PLA and PETG are miscible when PETG contents are below 22 wt%. In accordance with this result, the tan δ peak and glass transition temperatures of blends determined from dynamic mechanical analysis (DMA) and differential scanning calorimetry (DSC) showed a single peak at PETG contents lower than 22 wt%. Tensile test results showed that the elongation at the break of blends increased with an increase in PETG content. DSC and isothermal crystallization results showed that PETG accelerates the crystallization rate of PLA at PETG contents lower than 22 wt%, indicating that PETG acts as a nucleation agent in the crystallization of PLA. Wide angle X-ray diffraction results (WAXD) showed that the crystalline structure of PLA is not affected by the incorporation of PETG.

Keywords: poly(lactic acid), poly(ethylene terephthalate glycol), blends, compatibility, physical properties.

Introduction

Poly(lactic acid) (PLA) is one of the most promising bio-based plastics in biomedical and other industrial fields due to its good biocompatibility and mechanical properties compared with other biodegradable polymers.[1-3] However, defects in physical properties such as brittleness, low thermal stability, and low crystallization rate limit the applications of PLA.

Considerable research has been carried out to overcome the shortcomings of PLA by compounding PLA with nanomaterials,[4-7] copolymerization,[8-11] and blending with other polymers.[12-16] Among these strategies, blending of PLA with other biodegradable polymers such as poly(ε-caprolactone) (PCL),[12] poly(ethylene glycol) (PEG),[13] poly(propylene glycol) (PPG),[14] poly(butylene adipate-*co*-terephthalate) (PBAT),[15] and poly(butylene succinate) (PBS)[16] have proven attractive to improve biodegradability, processability, and toughness. Sheth *et al.*[13] reported that PLA/PEG blends exhibited enhanced crystallization and biodegradability compared to neat PLA. Jiang *et al.*[15] reported that PLA blending with PBAT improved the processability, toughness, and crystallization of PLA. Both PEG and PBAT act as plasticizers in PLA, resulting that the glass transition temperatures of the blends were decreased. The elongation at break of theses blends was improved but the tensile strength and modulus were significantly decreased, consequently, the applications of such blends are limited.

Poly(ethylene terephthalate glycol) (PETG), generally described as poly(ethylene-*co*-1,4-cyclohexane dimethanol terephthalate), is a random copolymer of poly(ethylene terephthalate) (PET) with an additional 30-34 mol% of 1,4-cyclohexane dimethanol (CHDM), as shown in Scheme I.[17] The crystallinity of PETG is extremely low due to steric hindrance of the CHDM groups, but PETG has good flexibility, toughness, and processability.[18] In particular, the processing temperature of PETG is similar to that of PLA. Taking these advantages into consideration, PLA blending with PETG using melt compounding can be effective to overcome the drawbacks of PLA, resulting that PLA/PETG blends are more widely used in packaging industries. However, the compatibility and the physical properties of the PLA/PETG blends have not been reported in the literature.

We prepared PLA/PETG blends with various mixture

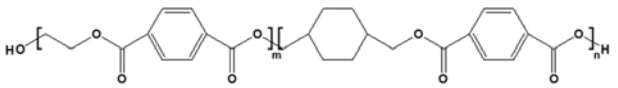

Scheme I. The structure of PETG.

*Corresponding Author. E-mail: imss007@hanyang.ac.kr

ratios and predicted the compatibility between PLA and PETG using interaction parameters derived from difference between the solubility parameters of two polymers and Flory-Huggins theory based on the melting temperature depression. The main objective of this study is to investigate how changes in PETG content affect the physical properties and isothermal crystallization behaviors of the blends.

Experimental

Materials. PLA was purchased from Nature Works®, and is a semicrystalline grade (PLA 4032D) with a D-isomer content of 1.2-1.6 mol%. PETG (SKYGREEN®, KN100) was supplied by SK Chemicals. Both polymers were supplied in pellet form. The number-average molecular weight and polydispersity of PLA and PETG are listed in Table I. PLA and PETG were used after drying under vacuum at 65 and 80 °C for 1 day, respectively.

Sample Preparation of Blends. PLA and PETG were melt-blended using a twin counter-rotating mixer (Thermo Haake co.) at 200 °C for 1 min at 200 rpm in the ratios of 100/0, 98/2, 90/10, 80/20, 70/30, 60/40, and 50/50 (PLA/PETG). Films were prepared for mechanical testing using a compression molding hot-press at 200 °C and a pressure of 4,000 psi for 5 min to produce uniform films (20 cm×20 cm ×0.4 mm). The prepared films were rapidly transferred to ice water for quenching, and dried under vacuum at 65 °C for 1 day to thoroughly remove water. The sample code is denoted by the PLA and PETG composition. For example, 8020 is made up of 80 wt% PLA and 20 wt% PETG.

Characterization. Dynamic mechanical properties were determined by dynamic mechanical analysis (DMA, DMA2980; TA Instruments, New Castle, DE, USA). The measurements were performed using a tension mode at a frequency of 3 Hz under a nitrogen atmosphere and the samples were heated gradually from 30 to 150 °C at a rate of 2 °C/min. Mechanical tests were conducted using a tensile test machine (Instron 4465; Instron Corp., Norwood, MA, USA) with a crosshead speed of 10 mm/min at room temperature. Both the thermal properties and isothermal crystallization behaviors of PLA/PETG blends were conducted using differential scanning calorimetry (DSC, Perkin-Elmer DSC 7, Perkin-Elmer, Wellesley, MA, USA). For isothermal crystallization behavior, the samples were quenched to the desired crystallization temperature (95, 100, 105, and 115 °C) after elimination of the thermal history. After crystallization, the sample was quenched at 30 °C, and then a second heating was conducted at a heating rate of 10 °C/min. Spherulite morphologies of PLA/PETG blends were observed using a polarizing optical microscope (POM, U-AN360P; Olympus. Tokyo, Japan) equipped with a CCD camera. First, a 3 mg sample was placed between two glass coverslips and was melted on a hot plate at 200 °C for 2 min. Then, the samples were quickly transferred to an FP82HT hot stage (Mettler-Toledo, Columbus, OH, USA) and were held at 95 and 115 °C for 20 min. Wide angle X-ray diffraction (WAXD) was conducted with CuK_α radiation (λ=1.54 Å) on an X-ray generator (Rigaku RINT 2000; Rigaku Corp., Tokyo, Japan) operating 40 kV and 100 mA from 5° to 40° at scan rate 7°/min after the samples were treated to 130 °C for 6 h to confirm the effect of PETG on crystal structure of PLA.

Table I. The Number-Average Molecular Mass and Polydispersity of PLA and PETG

	M_n	M_w/M_n
PLA	119,000	1.74
PETG	28,000	2.50

Results and Discussion

The compatibility between two polymers is the most important factor to develop optimum properties in a blend system and compatibility can be predicted by the variation in the Gibbs' free energy of mixing (ΔG_{mix}) using the volume fraction of the two polymers. The Gibbs' free energy of mixing is calculated using the Flory-Huggins theory as following equation:

$$\frac{\Delta G_{mix}}{RT} = \frac{\phi_1}{m_1}\ln\phi_1 + \frac{\phi_2}{m_2}\ln\phi_2 + \chi_{12}\phi_1\phi_2 \quad (1)$$

where T is the temperature, R is the gas constant, m is degree of polymerization, ϕ is volume fraction, and χ_{12} is interaction parameter, and the subscripts 1 and 2 refer to PLA and PETG, respectively.[19] Generally, the entropy term due to statistical thermodynamics in polymer-polymer mixture systems is very small because of a much lower number of possible arrangements compared with those in solvent-solvent or solvent-polymer mixtures systems.[20] For this reason, the Gibbs' free energy of mixing is strongly dependent on the interaction parameter (χ_{12}) in the blend system.

We predicted compatibility using the interaction parameter between PLA and PETG derived from the difference in the solubility parameters (δ), according to following equation:

$$\chi_{12} = (\delta_1 - \delta_2)^2 \times \frac{V_c}{RT} \quad (2)$$

where V_c is the molar volume of the reference unit, which is taken as close to the molar volume of the smallest polymer repeat unit; it is often arbitrarily set to 100 cm^3/mol.[21] Although eq. (2) cannot provide negative values of the interaction parameter, we can still conclude that very small value or zero of (δ_1-δ_2) indicates that the two polymers are more compatible. The calculated solubility parameters of PLA and PETG using various group contribution methods are listed in Table II. As a result, the difference between the solubility parameters of the two polymers is in the range from 0.06 to 0.55, indicating that there is no great difference

Table II. The Solubility Parameters Calculated from Group Contribution Method of PLA and PETG

	Fedors	Hoftyzer & Van Krevelen				Hoy			
	δ	δ_t	δ_d	δ_p	δ_h	δ_t	δ_d	δ_p	δ_h
PLA	21.88	21.15	14.65	9.70	11.77	22.25	15.28	11.91	8.73
PETG	21.94	20.60	17.88	4.31	9.22	22.65	16.61	12.00	8.88

between them.

The compatibility is more clearly determined using the interaction parameter derived from the Flory-Huggins theory based on the melting temperature depression. First, we estimated the equilibrium melting temperature (T_m^0) using the Hoffman-Week equation to determine interaction parameter:

$$T_m = \frac{T_c}{\gamma} + \left(1 - \frac{1}{\gamma}\right) T_m^0 \quad (3)$$

where T_m is the experimental melting temperature and γ is the lamellar thickening coefficient.[22] According to this equation, T_m^0 is derived from the intersection between the linear extrapolation of the observed T_m as a function of crystallization temperature and line T_m=T_c. Figure 1 shows the Hoffman-Weeks plots of PLA/PETG blends. In Figure 1, T_m^0 of neat PLA used in this work was 201.7 °C, which is slightly lower than previously reported values in the range from 207 to 212 °C.[23] When PETG contents are lower than 20 wt%, the T_m^0 decreased with increasing PETG content, and the lowest T_m^0 is 185.6 °C in a 8020 blend. On the other hands, the T_m^0 increased slightly at PETG contents higher than 20 wt%.

According to Flory-Huggins theory, the interaction parameter is calculated using the following equation:

$$\chi_{12}\phi_2^2 = -\left[\frac{\Delta H^0 V_2}{R V_1}\left(\frac{1}{T_m^0(blend)} - \frac{1}{T_m^0(pure)}\right) + \frac{\ln\phi_1}{m_1} + \left(\frac{1}{m_1} - \frac{1}{m_2}\right)\phi_2\right] \quad (4)$$

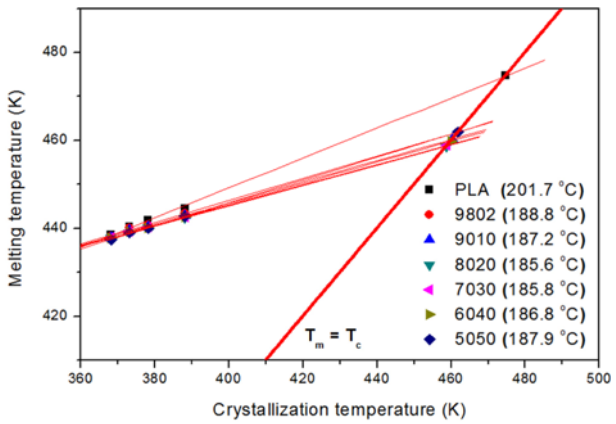

Figure 1. Equilibrium melting temperature of PLA/PETG blends by using Hoffman-Weeks plot.

Table III. The Parameter Values of PLA and PETG for Using Flory-Huggins Equation

	PLA	PETG
m^a	1,639	128
V^b (V/mol)	50.5	172.0
d (g/cm^3)	1.25	1.27

[a]m: Degree of polymerization. [b]V: Molar volume.

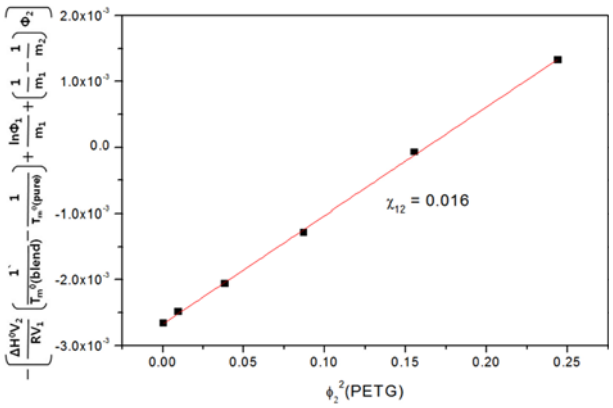

Figure 2. Plot according to Flory-Huggins equation for PLA/PETG blends at various compositions.

where m and ϕ are the same values as in eq. (1), ΔH^0 is the enthalpy of fusion per mole of repeat unit, and V is the molar volume of the repeating unit. In eq. (4), the interaction parameter is calculated using the slope of a plot of the right side of the equation *vs.* ϕ_2^2. The values of m and V are listed in Table III and Hoffman *et al.*[24] reported that the ΔH^0 of PLA is 120 J/g. Figure 2 shows a plot of PLA/PETG blends using eq. (4). In Figure 2, the interaction parameter between PLA and PETG derived from Flory-Huggins theory was 0.016. This result indicates that the PLA/PETG blend was adjacent to a compatible phase.

We determined the phase behavior of PLA/PETG blends using eq. (1) and the interaction parameter derived from the Flory-Huggins theory. Figure 3 shows the phase diagram of PLA/PETG blends. The marked points indicate the Gibbs' free energy of mixing versus the volume fraction of PETG calculated from the weight percentage and density. Although a negative value of the Gibbs' free energy of mixing is not a sufficient condition for miscibility between the two polymers, the phase diagram derived from the Gibbs' free energy of

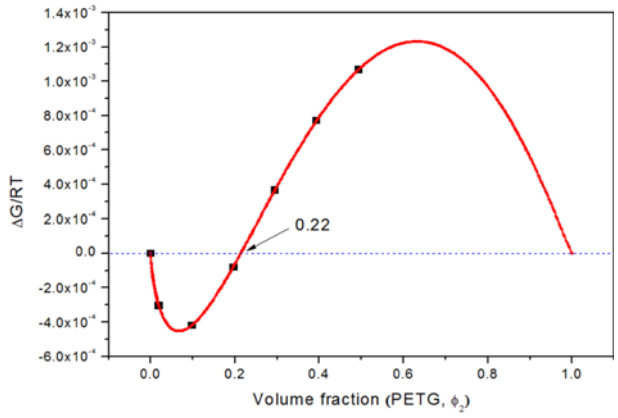

Figure 3. Phase diagram of PLA/PETG blends.

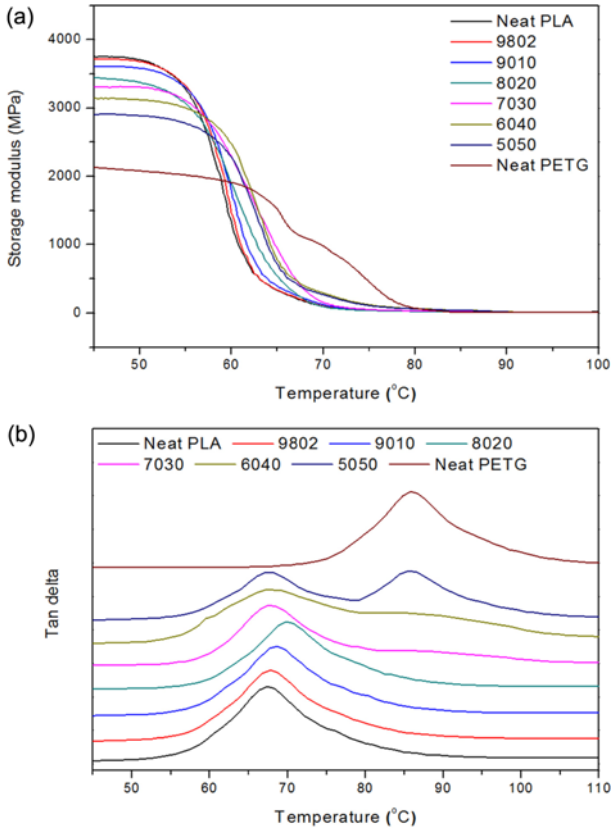

Figure 4. The storage modulus (a) and tan δ peak (b) of PLA/PETG blends.

mixing provides a good prediction for determining the miscibility. As a result, in Figure 3, the Gibbs' free energy of mixing became positive at over 22 wt% PETG content, indicating that PLA/PETG blends are miscible at PETG contents lower than 22 wt%.

Figure 4 shows the storage moduli and tan δ peaks of various samples. In Figure 4(a), the storage moduli of blends decreased with an increase in PETG content, indicating that PETG reduced the stiffness of PLA. In Figure 4(b), the tan δ peak temperatures of neat PLA and PETG are 67.3 and 85.7 °C, respectively. When PETG content is lower than 20 wt%, the tan δ peak temperatures of the blends were single and slightly increased with increasing PETG content. On the other hand, two glass transitions are shown at PETG contents higher than 20 wt%. Considering these results, the PLA/PETG blends are miscible at PETG contents lower than 20 wt%, which is consistent with the phase diagram result.

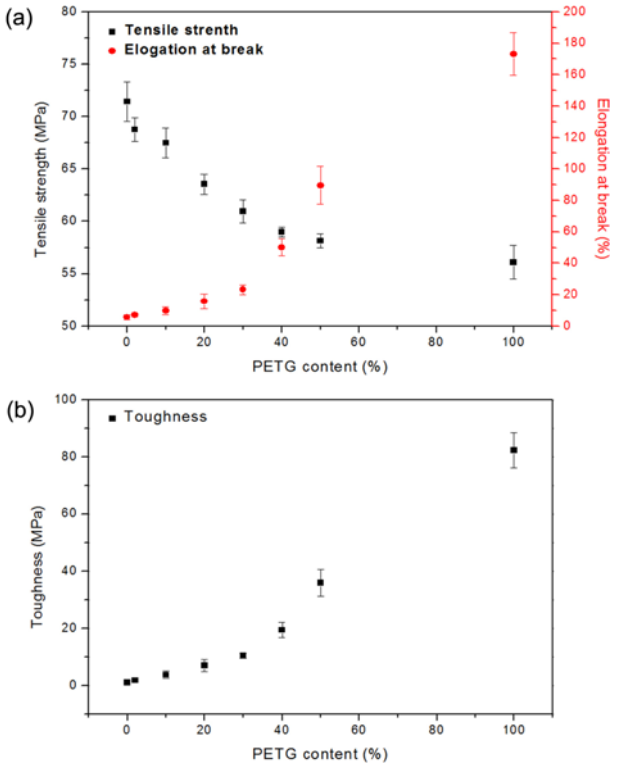

Figure 5. The mechanical properties of PLA/PETG blends versus PETG content: (a) tensile strength and elongation at break and (b) toughness.

Figure 5 displays the tensile strength, elongation at break, and toughness of PLA/PETG blends versus PETG content. In Figure 5(a) and (b), neat PLA exhibited low elongation at break (5.7%) and toughness (1.0 MPa) due to brittleness. In contrast, the elongation at break and toughness of blends increased with the an increase in PETG content but the tensile strength of the blends decreased because that of neat PETG is lower than neat PLA. Although compatibility between the two polymers is most important factor with respect to the blend properties, the mechanical test results showed that changes in the mechanical properties of blends were not largely dependent on the compatibility between them. Compared with neat PLA, the elongation at break and toughness of the 9010 blend increased about 170% (68.8 MPa) and 370% (3.7 MPa), respectively. As a result, regardless of the compatibility, an improvement in the toughness of PLA

Table IV. Thermal Properties of PLA/PETG Blends[a]

Sample Code	T_{g1} (°C)	T_{g2} (°C)	T_{cc} (°C)	ΔH_{cc} (J/g)	T_{m1} (°C)	T_{m2} (°C)	ΔH_m (J/g)	X_c (%)	T_m^0 (°C)
Neat PLA	61.0	-	129.6	35.2	167.0	-	38.9	41.8	201.7
9802	61.2	-	129.2	34.9	166.8	-	38.8	42.6	188.8
9010	61.3	-	128.4	33.7	166.6	-	36.4	43.5	187.2
8020	61.6	-	122.7	31.6	165.4	-	33.5	45.0	185.6
7030	61.4	78.8	127.6	25.2	166.1	-	27.0	41.5	185.8
6040	61.3	79.2	129.3	20.5	166.0	-	22.1	39.6	186.8
5050	61.1	79.3	117.1	14.2	164.4	169.0	16.1	34.6	187.9
Neat PETG	-	79.5	-	-	-	-	-	-	-

[a]Note: Heating and cooling rate: 10 °C/min.

was achieved with the addition of PETG, indicating that PETG plays a role as a plasticizer of PLA and the brittle fracture of neat PLA was changed to ductile fracture of blends with the addition of PETG.

The thermal characteristic values determined from DSC measurements are summarized in Table IV. Neither PLA nor PETG exhibited crystallization peaks during cooling due to the slow crystallization rate of PLA and PETG. In accordance with these facts, no samples exhibited crystallization peaks during cooling. The glass transition temperatures (T_g) of neat PLA and PETG are 61.0 and 79.5 °C, respectively. T_g values of the blends were single and slightly increased at PETG contents lower than 20 wt% while two glass transitions were shown between the T_g values of PLA and PETG above 20 wt% PETG content, which is consistent with the DMA results. The melting temperatures (T_{m1}) of blends depressed with increasing PETG content. Generally, the melting temperature of the blend is lower than that of the pure polymer in miscible or compatible blend systems.[25] In particular, the increase in PETG content brought about a melting shoulder at temperature higher than T_{m1}. For 5050 blend, the melting peak clearly separated into two individual peaks. This phenomenon could be mainly attributed to the crystalline PLA because the crystallization rate of PLA is much faster than that of PETG. However, Kattan *et al.* reported that PETG can crystallize after isothermal crystallization at 120 °C for 48 h and the melting temperature of this crystalline phase is 163 °C.[26] Therefore, the effect of PETG on the melting behaviors of the blends cannot be neglected and will be described in detail in a future paper. The heat of fusion is largely dependent on PLA because neat PETG did not show the crystallization and melting peaks during measurements. Therefore, the degree of crystallinity (X_c) of PLA and the blends are calculated from the following equation:

$$X_c\ (\%) = \frac{\Delta H_f}{\omega_{PLA} \times \Delta H_f^0} \times 100 \quad (5)$$

where ΔH_f is the heat of fusion of PLA/PETG blends and ω_{PLA} is the weight fraction of PLA in the blends. Further, ΔH_f^0 is the heat of fusion for 100% crystalline PLA, 93.0 J/g.[27] When PETG contents of PLA/PETG blends were lower than 20 wt%, the cold crystallization temperature (T_{cc}) shifted to a lower temperature, the peak width narrowed, and X_c increased with increasing PETG content, indicating that blending with PETG improved the crystallization ability of PLA by acting as a nucleation agent with PETG contents lower than 20 wt%.

Isothermal crystallization was conducted to describe the nucleation effect of PETG in PLA/PETG blends with lower than 20 wt% PETG content. Then, we analyzed the crystallization kinetics and the half-time of crystallization using the Avrami equation.[28,29] The Avrami exponent (n) and kinetic rate constant (k) are obtained from the slope and intercept of a linear plot of $\log(-\ln(1-X_t))$ against $\log(t)$ in the primary crystallization portion. The Avrami parameters derived from the isothermal crystallization measurements are summarized in Table V. With a decrease in the isothermal crystallization temperature and an increase in the content of PETG, the half-time of crystallization ($t_{1/2}$) decreased and the kinetic rate constant increased, especially the half-time of the crystallization and the kinetic rate constant of the 8020 blend were the fastest and highest values among the samples at a designated isothermal crystallization temperature, indicating that PETG acts as a nucleation agent for the crystallization of PLA/PETG blends.

Figure 6 shows spherulite morphologies of PLA/PETG blends with PETG contents lower than 20 wt% after isothermal crystallization at 95 and 115 °C for 20 min. The size and density of spherulites increased with increasing PETG content as well as decreasing the isothermal crystallization temperature. This result also supports the above explanation that PETG can act as the nucleation agent.

Figure 7 shows the WAXD profiles of neat PLA, 8020 blend, and neat PETG. All samples were amorphous in a quenched state for preparing films. We treated the samples

Table V. Avrami Parameters for the Isothermal Crystallization of PLA/PETG Blends

Sample Code	95 °C			100 °C			105 °C			115 °C		
	n	$k\times10^{-2}$	$t_{1/2}$ (min)	n	$k\times10^{-2}$	$t_{1/2}$ (min)	n	$k\times10^{-2}$	$t_{1/2}$ (min)	n	$k\times10^{-2}$	$t_{1/2}$ (min)
Neat PLA	2.4	0.91	6.1	2.4	0.55	7.6	2.5	0.20	10.4	2.5	0.12	12.3
9802	2.2	1.87	5.2	2.5	0.63	6.7	2.6	0.29	8.3	2.5	0.23	10.2
9010	2.1	2.80	4.7	2.3	1.21	5.8	2.3	0.67	7.4	2.3	0.48	8.7
8020	2.1	4.70	3.7	2.2	2.12	4.9	2.1	1.53	6.0	2.4	0.57	7.2

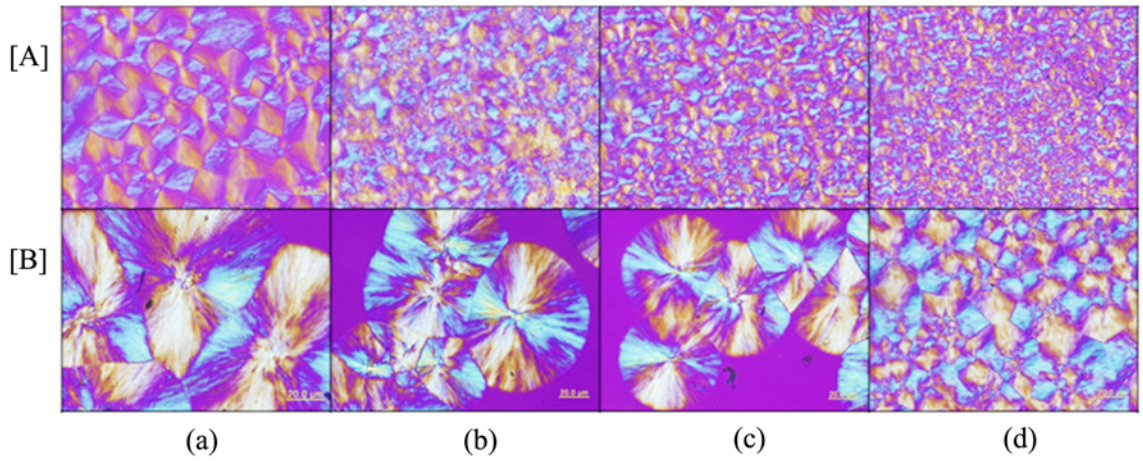

Figure 6. Micrographs of spherulite morphologies from (a) PLA, (b) 9802, (c) 9010, and (d) 8020 for 20 min at [A] 95 °C and [B] 115 °C.

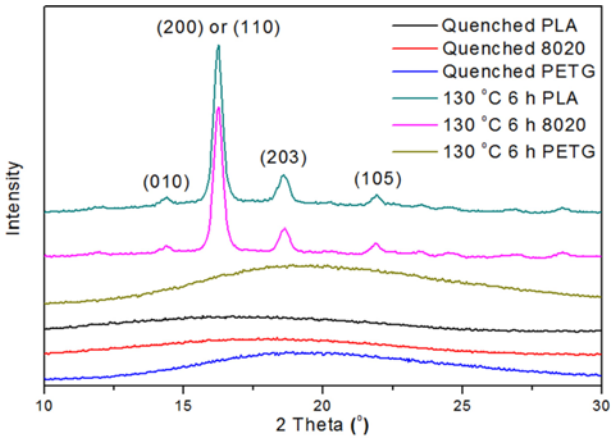

Figure 7. WAXD profiles of neat PLA, 8020 blend and neat PETG.

at 130 °C for 6 h to confirm the effects of PETG on the crystalline structure of PLA. In Figure 7, neat PLA and 8020 blend were sufficiently crystallized. On the other hands, neat PETG did not exhibit a crystallization peak. Neat PLA exhibits X-ray diffraction peaks at 14.3°, 16.2°, 18.6°, and 21.9°, corresponding to crystallographic plan indexes of (010), (200)/(110), (203), and (105), respectively.[30] Compared to neat PLA, the location of the characteristic peaks of the 8020 blend was unchanged even though PETG was incorporated, indicating that PETG did not affect the crystalline structure of PLA.

Conclusions

We successfully prepared PLA/PETG blends using melt compounding with various composition. The interaction parameter between PLA and PETG derived from Flory-Huggins theory predicted that PLA and PETG are miscible at PETG contents lower than 22 wt%. In accordance with this result, the tan δ peak temperatures and glass transition temperatures determined from the DMA and DSC are single and slightly increased with increasing PETG content at PETG contents lower than 22 wt%. The toughness of the blends increased with increasing PETG content regardless of the compatibility between PLA and PETG, indicating that improvement in the toughness of PLA was achieved with the addition of PETG. In particular, when content of PETG was lower than 22 wt%, the half-time of crystallization ($t_{1/2}$) decreased and the kinetic rate constant (k) increased with increasing PETG content, indicating that PETG acts as a nucleation agent for the isothermal crystallization of PLA. The WAXD results showed that the crystal structure of PLA was not affected by the incorporation of PETG.

References

(1) R. E. Drumright, P. R. Gruber, and D. E. Henton, *Adv. Mater.*, **12**, 1841 (2000).
(2) R. Auras, B. Harte, and S. Selke, *Macromol. Biosci.*, **4**, 835

(2004).
(3) F. Carrasco, P. Pagés, J. Gámez-Pérez, O. O. Santana, and M. L. Maspoch, *Polym. Degrad. Stab.*, **95**, 116 (2010).
(4) S. Yan, J. Yin, Y. Yang, Z. Dai, J. Ma, and X. Chen, *Polymer*, **48**, 1688 (2007).
(5) S. S. Ray, P. Maiti, M. Okamoto, K. Yamada, and K. Ueda, *Macromolecules*, **35**, 3104 (2002).
(6) Y. S. Yun, H. I. Kwon, H. Bak, E. J. Lee, J. S. Yoon, and H. J. Jin, *Macromol. Res.*, **18**, 828 (2010).
(7) H. Pan and Z. Qiu, *Macromolecules*, **43**, 1499 (2010).
(8) M. Hiljanen-Vainio, P. A. Orava, and J. V. Seppala, *J. Biomed. Mater. Res.*, **34**, 39 (1997).
(9) J. Kylmä and J. V. Seppälä, *Macromolecules*, **30**, 2876 (1997).
(10) N. Kawasaki, A. Nakayama, Y. Maeda, K. Hayashi, N. Yamamoto, and S. Aiba, *Macromol. Chem. Phys.*, **199**, 2445 (1998).
(11) W. Li, J. Zeng, Y. Li, X. Wang, and Y. Wang, *J. Polym. Sci. Part A: Polym. Chem.*, **47**, 5898 (2009).
(12) H. Tsuji and G. Horikawa, *Polym. Int.*, **56**, 258 (2007).
(13) M. Sheth, R. A Kumar, V. Davé, R. A. Gross, and S. P. McCarthy, *J. Appl. Polym. Sci.*, **66**, 1495 (1997).
(14) Z. Kulinski, E. Piorkowska, K. Gadzinowska, and M. Stasiak, *Biomacromolecules*, **7**, 2128 (2006).
(15) L. Jiang, M. P. Wolcott, and J. Zhang, *Biomacromolecules*, **7**, 199 (2006).
(16) S. B. Park, S. Y. Hwang, C. H. Moon, S. S. Im, and E. S. Yoo, *Macromol. Res*., **18**, 463 (2010).
(17) K. J. Saunders, *Organic Polymer Chemistry: An Introduction to the Organic Chemistry of Adhesives*, Chapman and Hall, London, 1988.
(18) A. Ranade, N. D'Souza, C. Thellen, and J. A. Ratto, *Polym. Int.*, **54**, 875 (2005).
(19) P. J. Flory, *Principles of Polymer Chemistry*, Cornell Univ. Press, Ithaca, New York, 1953.
(20) L. M. Robeson, *Polymer Blends: A Comprehensive Review*, Hanser Gardner Publications, Cincinnati, 2007.
(21) J. H. Hildebrand and R. L. Scott, *The Solubility of Nonelectrolytes*, 3rd ed., Reinhold, New York, 1950.
(22) J. D. Hoffman and J. J. Weeks, *J. Res. Natl. Bur. Stand A*, **66**, 13 (1962).
(23) H. Tsuji and Y. Ikada, *Polymer*, **36**, 2709 (1995).
(24) J. D. Hoffman, R. L. Miller, H. Marand, and D. B. Roitman, *Macromolecules*, **25**, 2221 (1992).
(25) T. Nishi and T. T. Wang, *Macromolecules*, **8**, 909 (1975).
(26) M. Kattan, E. Dargent, J. Ledru, and J. Grenet, *J. Appl. Polym. Sci.*, **81**, 3405 (2001).
(27) E. W. Fisher, H. J. Sterzel, and G. Wegner, *Polymer*, **251**, 980 (1973).
(28) M. Avrami, *J. Chem. Phys.*, **9**, 177 (1941).
(29) M. Avrami, *J. Chem. Phys.*, **7**, 1193 (1939).
(30) J. F. Mano, Y. Wang, J. C. Viana, Z. Denchev, and M. J. Oliveira, *Macromol. Mater. Eng.*, **289**, 910 (2004).